



# Myocardial perfusion impairment in children with Kawasaki disease: assessment with cardiac magnetic resonance first-pass perfusion

Zhongqin Zhou<sup>1,2#</sup>, Nanjun Zhang<sup>3,4#</sup>, Shiganmo Azhe<sup>1,2</sup>, Lei Hu<sup>1,2</sup>, Shengkun Peng<sup>5</sup>, Yingkun Guo<sup>1,2</sup>, Kaiyu Zhou<sup>2,3,6</sup>, Chuan Wang<sup>2,3,6</sup>, Lingyi Wen<sup>1,2</sup>

<sup>1</sup>Department of Radiology, West China Second University Hospital, Sichuan University, Chengdu, China; <sup>2</sup>Key Laboratory of Birth Defects and Related Diseases of Women and Children (Sichuan University), Ministry of Education, West China Second University Hospital, Sichuan University, Chengdu, China; <sup>3</sup>Department of Pediatric Cardiology, West China Second University Hospital, Sichuan University, Chengdu, China; <sup>4</sup>West China Medical School of Sichuan University, Chengdu, China; <sup>5</sup>Department of Radiology, Sichuan Academy of Medical Sciences and Sichuan Provincial People's Hospital, University of Electronic Science and Technology of China, Chengdu, China; <sup>6</sup>Key Laboratory of Development and Diseases of Women and Children of Sichuan Province, West China Second University Hospital, Sichuan University, Chengdu, China

*Contributions:* (I) Conception and design: Z Zhou, Y Guo, L Wen; (II) Administrative support: K Zhou, C Wang; (III) Provision of study materials or patients: Y Guo, K Zhou, C Wang, L Wen; (IV) Collection and assembly of data: Z Zhou, N Zhang, S Azhe, L Hu, S Peng; (V) Data analysis and interpretation: Z Zhou, N Zhang; (VI) Manuscript writing: All authors; (VII) Final approval of manuscript: All authors.

#These authors contributed equally to this work.

*Correspondence to:* Lingyi Wen, PhD. Department of Radiology, West China Second University Hospital, Sichuan University, No. 20, Section 3, Renmin South Road, Chengdu 610041, China; Key Laboratory of Birth Defects and Related Diseases of Women and Children (Sichuan University), Ministry of Education, West China Second University Hospital, Sichuan University, Chengdu, China. Email: lizzievane@126.com; Chuan Wang, PhD. Department of Pediatric Cardiology, West China Second University Hospital, Sichuan University, No. 20, Section 3, Renmin South Road, Chengdu 610041, China; Key Laboratory of Birth Defects and Related Diseases of Women and Children (Sichuan University), Ministry of Education, West China Second University Hospital, Sichuan University, Chengdu, China; Key Laboratory of Development and Diseases of Women and Children of Sichuan Province, West China Second University Hospital, Sichuan University, Chengdu, China. Email: 805101396@qq.com.

**Background:** Kawasaki disease (KD) potentially increases the risk of myocardial ischemia. This study aimed to semi-quantitatively evaluate myocardial perfusion impairment using cardiac magnetic resonance (CMR) first-pass perfusion in children with KD and explore the association between coronary artery (CA) dilation and myocardial perfusion.

**Methods:** From December 2018 to July 2021, 77 patients with KD (48 male, 5.71±2.80 years) and 37 age- and sex-matched normal controls (20 male, 6.19±3.32 years) who underwent CMR in West China Second University Hospital were enrolled in this cross-sectional study with prospective data collection. A total of 30 of these patients completed the follow-up CMR, with a median interval of 13 months. Myocardial perfusion parameters including perfusion index (PI) and maximum signal intensity (Max SI) were obtained through rest first-pass perfusion. The internal diameter of the CA was assessed via coronary magnetic resonance angiography (CMRA) to calculate the coronary Z score. The global and regional myocardial parameters among the subgroups were compared. Statistical analysis included one-way analysis of variance (ANOVA), Pearson's correlation, and multivariate linear regression.

**Results:** The global Max SI and regional Max SI of all segments in patients with and without CA dilation decreased compared with those in controls (P=0.19 and P<0.001, respectively). The global PI of patients with CA dilation and regional PI in segments subtended by dilated CA were lower than that of controls (P=0.002 and P<0.001, respectively) and were negatively correlated with the Z score (global: r=-0.576; regional: r=-0.351, both P<0.001). Multivariate analysis revealed that the Z score was negatively associated with global

PI in KD ( $\beta=-0.409$ ,  $P=0.02$ , model  $R^2=0.170$ ). The global Max SI of patients with and without CA dilation during the follow-up CMR decreased compared with that of the first CMR ( $42.18\pm 9.84$  vs.  $34.48\pm 8.24$ ,  $P=0.02$ ;  $44.82\pm 7.13$  vs.  $36.61\pm 7.67$ ,  $P=0.03$ , respectively).

**Conclusions:** CMR myocardial first-pass perfusion imaging can semi-quantitatively evaluate impaired myocardial perfusion in KD patients. Not only patients with CA dilation and segments subtended by dilated CA but also those without CA dilation and segments subtended by non-dilated CA developed myocardial perfusion impairment, the severity of myocardial perfusion impairment is associated with the degree of CA dilation.

**Keywords:** Kawasaki disease (KD); cardiac magnetic resonance (CMR); myocardial perfusion impairment; coronary artery dilation (CA dilation)

Submitted Dec 19, 2023. Accepted for publication Jun 03, 2024. Published online Jun 27, 2024.

doi: 10.21037/qims-23-1802

View this article at: <https://dx.doi.org/10.21037/qims-23-1802>

## Introduction

Kawasaki disease (KD) is an illness characterized by acute febrile episodes and systemic vasculitis that predominantly occur in infants and children (1,2). KD affects small- and medium-sized arteries, particularly the coronary artery (CA), causing CA lesions ranging from dilation to giant coronary aneurysm (CAA) (3). It has become the most common cause of acquired coronary artery disease in children in developed countries (1,2).

CA dilation is the most important cardiovascular sequela at the acute stage and follow-up in patients with KD (2,3). However, several studies have shown that among patients with KD, both those with CA dilation and those without develop myocardial perfusion impairment (4-8). In the absence of epicardial CA lesions, these findings may indicate underlying myocardial microcirculation dysfunction (6). There are multiple modalities that can semi-quantitatively or quantitatively evaluate myocardial perfusion. These include intracoronary Doppler (9), positron emission tomography (PET) (4,10-12), single-photon emission computed tomography (SPECT) (5), and cardiac magnetic resonance (CMR) first-pass perfusion (6-8). In children, the application of intracoronary Doppler, PET, and SPECT is limited due to invasiveness and radiation exposure (13).

CMR has significantly superior spatial resolution and temporal resolution to those of PET and SPECT (14). Further, it can facilitate the evaluation of anatomical and tissue characteristics noninvasively and without radiation exposure. Thus, it is suitable for perfusion assessment in children. To the best of our knowledge, only 3 studies have performed semi-quantitative or quantitative CMR perfusion

evaluation in patients with KD (6-8). However, these studies did not include an age-matched pediatric control group and follow-up of a large number of participants. In addition, they did not fully elucidate the correlation between myocardial perfusion impairment and CA dilation. Therefore, the current study aimed to semi-quantitatively evaluate myocardial perfusion impairment and the change in myocardial perfusion during follow-up via myocardial first-pass perfusion CMR in patients with KD. Further, the association between myocardial perfusion and CA dilation was evaluated. We present this article in accordance with the STROBE reporting checklist (available at <https://qims.amegroups.com/article/view/10.21037/qims-23-1802/rc>).

## Methods

### Study population

This cross-sectional study was performed in accordance with the Declaration of Helsinki (as revised in 2013) and has been approved by Medical Ethics Committee of Sichuan University (No. K2019058). Written informed consent was obtained from the parents of all patients prior to study participation. The calculated sample size for this study was 76. This sample size was based on a 95% confidence level ( $\alpha=0.05$ ) and a 90% statistical power ( $\beta=0.10$ ). The inclusion criteria were patients diagnosed with KD (2). The exclusion criteria were patients with a history of other cardiovascular diseases; those with contraindications to MRI examination and gadolinium contrast agent; those with CA thrombosis and/or stenosis (diagnosed by echocardiology, coronary computed tomography angiography, or coronary magnetic

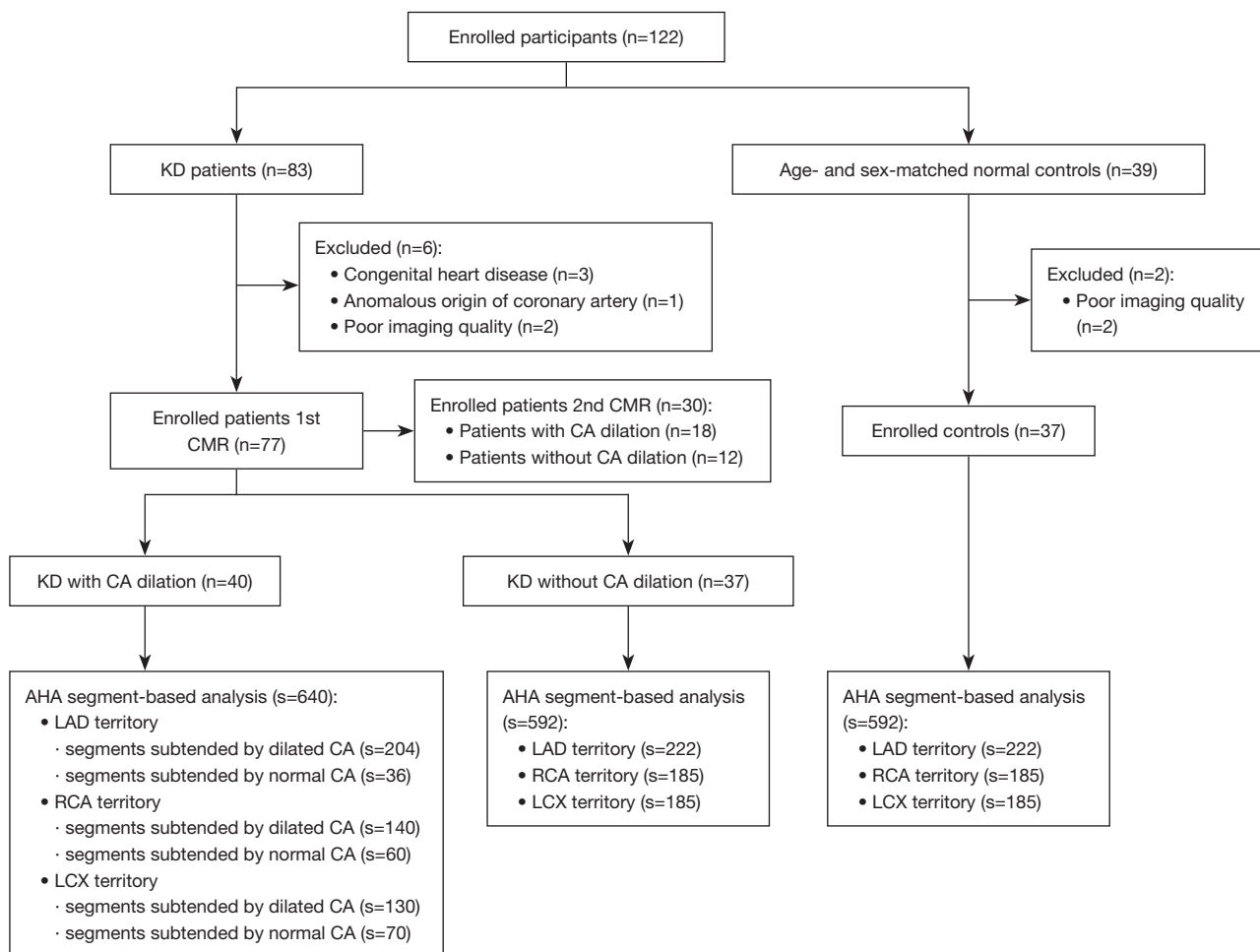


**Figure 1** Study flowchart. KD, Kawasaki disease; CMR, cardiac magnetic resonance; CA, coronary artery; AHA, American Heart Association; LAD, left anterior descending artery; RCA, right coronary artery; LCX, left circumflex artery; s, segments.

resonance); and those with uninterpretable images. From December 2018 to July 2021, 83 pediatric patients diagnosed with KD were prospectively recruited from West China Second University Hospital. After excluding 6 patients, 77 patients with KD (48 male,  $5.71 \pm 2.80$  years) were enrolled in this study (Figure 1); 30 of these patients completed the follow-up CMR. Meanwhile, 39 age- and sex-matched participants with suspected heart disease who underwent CMR during the same period but were finally diagnosed with normal conditions were included as controls. Among them, 2 subjects with images with uninterpretable quality were not included in the analysis.

### Image acquisition

CMR examinations were performed using a 3.0 T scanner

(Skyra; Siemens Medical Solutions, Erlangen, Germany) with an 18-channel coil. Patients who did not cooperate during MRI examination were performed under anesthesia. Informed consent was obtained from the parents of all of patients before examination. Patients were monitored by anesthesiologists during CMR examination. The CMR protocol included rest first-pass perfusion and coronary magnetic resonance angiography (CMRA). The acquisition of CMRA was performed using a T2-prepared segmented fast low-angle shot 3-dimensional spoiled gradient echo sequence with diaphragm navigator (15).

For first-pass perfusion imaging, 0.1 mL/kg of Gadobutrol (Gadovist; Bayer Healthcare Pharmaceuticals, Berlin, Germany) was administered at a rate of 1.5–2.0 mL/s using a power injector (Stellant; MEDRAD, Indianola, PA, USA). Then, 10 mL of saline was flushed at the same rate.

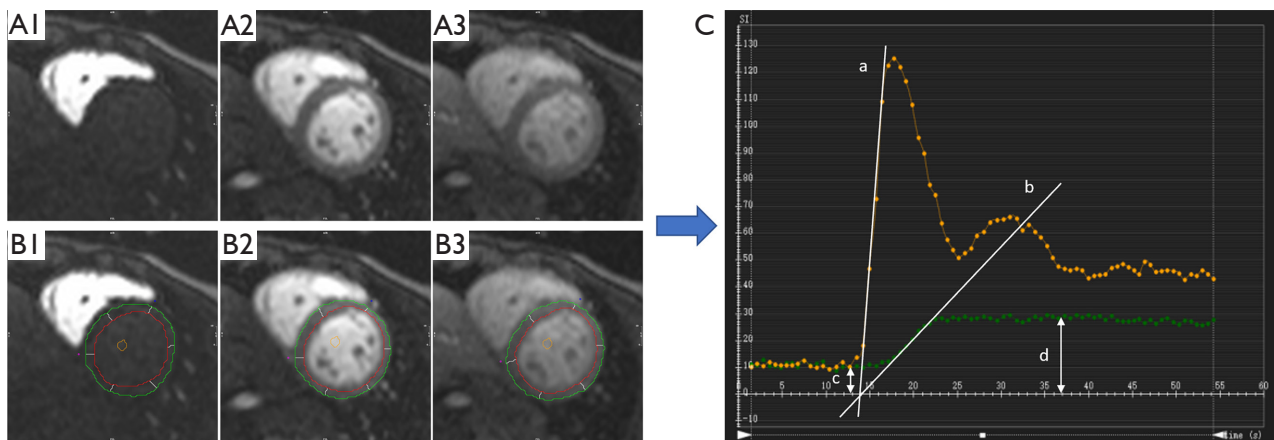


**Figure 2** Schematic diagram of postprocessing of CMR first-pass perfusion imaging. (A1-A3) Images of CMR first-pass perfusion sorted according to the time when the contrast agent through the myocardium. (B1-B3) Myocardial perfusion images show the region of interest of the myocardium (red for endocardium and green for epicardium) and blood pool (yellow) in image analysis. (C) Signal intensity-time curve derived from postprocessing software including: upslope<sub>max</sub> of blood pool (a), upslope<sub>max</sub> of myocardium (b), baseline of SI (c) and Max SI (d). CMR, cardiac magnetic resonance; SI, signal intensity; Max SI, maximum signal intensity.

Rest first-pass perfusion images were acquired in 3 short-axis slices (basal, middle, and apical) using an inversion recovery prepared echo-planar imaging sequence with the following parameters: repetition time, 2.0 ms; echo time, 1.1 ms; flip angle, 10°; field of view, 360×248 mm; slice thickness, 6 mm; and slice gap, 8–12 mm; inversion time: 95 ms; matrix size: 98×192. Each slice of perfusion images was completed in 80 cardiac cycles with 80 images, and an inline motion correction was applied after image acquisition to correct respiratory motion.

### Image analysis

Image analysis was performed by 2 radiologists (Z.Z. with 5 years of experience and A.S. with 3 years of experience) blinded to the characteristics of the patients using postprocessing software (CVI42, version 5.13.5; Circle Cardiovascular Imaging Inc., Calgary, AB, Canada). For first-pass perfusion, the endocardium and epicardium of the left ventricle (LV) and a region of interest drawn in the LV blood pool were manually defined in the perfusion images (basal, middle, and apical) (Figure 2). Then, the signal intensity-time curves were generated for 3 slices in the myocardium and blood pool and each myocardial segment based on the American Heart Association (AHA) 16-segment heart model (16). Finally, semi-quantitative perfusion parameters, including maximum signal intensity (Max SI) and perfusion index (PI), were

acquired automatically. PI is the ratio of upslope<sub>max</sub> in the myocardium and upslope<sub>max</sub> in the LV blood pool. The LV global Max SI and PI were calculated by obtaining the average values of the basal, middle, and apical slices.

For CMRA images, the evaluation of the inner diameter and the distribution of CA dilation in the right coronary artery (RCA) and left coronary artery (LCA) was performed based on axial images and curved planar reconstruction images. The Z score of the CA diameter of patients was calculated according to the inner diameter of CA, sex, height, and weight of the patients (17). CA dilation was defined as a Z score of  $\geq 2.0$  according to the scientific statement of KD issued by the AHA (2).

### Reproducibility of perfusion parameters

To assess intraobserver variability, the perfusion parameters of 20 random participants were measured again by 1 radiologist (Z.Z. with 5 years of experience) after 2 weeks. Interobserver variability was assessed using perfusion parameters obtained by the other radiologist (H.L. with 2 years of experience) who was blinded to these results.

### Statistical analysis

Statistical analysis was performed using the software SPSS 22.0 (IBM Corp., Armonk, NY, USA). Categorical variables were presented as numbers and percentages. For continuous

variables, the normality of the distribution was tested using Kolmogorov-Smirnov, and data were expressed as mean  $\pm$  standard deviation or median [interquartile range (IQR)] as appropriate. One-way analysis of variance (ANOVA) was performed to compare the global and regional semi-quantitative perfusion parameters. Moreover, the least-significant difference test was used to evaluate the difference among subgroups when the P value of one-way ANOVA was  $<0.05$ . The paired *t*-test was used to compare the global perfusion parameters between the first and follow-up CMR. Pearson's correlation was used to examine the correlation between the Z score and semi-quantitative perfusion parameters in patients with KD who had CA dilation. Spearman correlation was used to evaluate the association between KD and semi-quantitative perfusion parameters. Univariate and multivariate linear regression models were used to examine CA dilation and global PI in patients with KD during the first CMR and the difference value (D-value) of global PI between the first and follow CMR. Intra- and interobserver variabilities for reproducibility were assessed using the intraclass correlation coefficient (ICC). ICC was interpreted with:  $<0.50$ = poor;  $0.50 \leq \text{ICC} < 0.75$ = moderate;  $0.75 \leq \text{ICC} < 0.90$ = good;  $>0.90$ = excellent [95% confidence interval (CI) calculated from 2-way random-effects models] (18). All statistical tests were 2-tailed, and a P value of  $<0.05$  was considered statistically significant.

## Results

### *Characteristics of the participants*

The final cohort included 40 patients with CA dilation (28 male, average age  $6.07 \pm 3.20$  years), 37 without CA dilation (20 male, average age  $5.32 \pm 2.27$  years), and 37 controls (20 male, average age  $6.19 \pm 3.32$  years). Among patients who presented with CA dilation, 9 (22.5%) patients presented CA dilation to small CAA, 16 (40.0%) patients presented middle CAA, and 15 (37.5%) patients presented giant CAA; the median maximum diameter of CA in patients with CA dilation was 6.25 (4.63–8.85) mm, and the Z score was 7.25 (5.05–10.41); 22 (55.0%) patients had both RCA and LCA dilation, and 12 (30.0%) patients presented with LCA dilation and 6 (15.0%) with RCA dilation. During CMR evaluation, 27 (35.1%) patients were in acute stage, and 50 (64.9%) patients were in chronic stage. As depicted in *Table 1*, there were no significant differences in the baseline characteristics and LV function of patients with CA dilation, those without CA dilation, and normal controls (all  $P > 0.05$ ).

### *Global perfusion parameters*

The global Max SI of patients with and without CA dilation was lower than that of normal controls ( $41.14 \pm 10.51$  vs.  $41.48 \pm 9.71$  vs.  $47.58 \pm 12.49$ , respectively,  $P = 0.19$ ). However, there was no significant difference between patients with and without CA dilation. The global PI of patients with CA dilation was lower than that of normal controls ( $10.03 \pm 2.52\%$  vs.  $11.83 \pm 2.72\%$ ,  $P = 0.002$ ). *Figure 3* shows the representative CMRA, perfusion images and post-process perfusion images of controls and patients with and without CA dilation. *Figure 4* depicts the global perfusion parameters in detail. The diagnosis of KD was negatively correlated with global PI and Max SI (PI:  $r = -0.276$ ,  $P = 0.003$ ; Max SI:  $r = -0.225$ ,  $P = 0.02$ ).

### *Regional perfusion parameters*

For the left anterior descending artery (LAD) territory, the PI of segments subtended by dilated CA and segments subtended by normal CA in patients with CA dilation was lower than that of segments in patients without CA dilation and controls ( $12.80\% \pm 2.42\%$  vs.  $13.86\% \pm 4.14\%$  vs.  $15.01\% \pm 4.44\%$  vs.  $15.43\% \pm 3.89\%$ ,  $P < 0.001$ ). For the RCA territory, the PI of segments subtended by dilated CA was lower than that of segments in the other 3 subgroups ( $8.94\% \pm 2.62\%$  vs.  $11.98\% \pm 5.38\%$  vs.  $10.32\% \pm 3.10\%$  vs.  $11.18\% \pm 2.85\%$ ,  $P < 0.001$ ). The PI of segments in patients without CA dilation was lower than that of segments in controls ( $10.32\% \pm 3.10\%$  vs.  $11.18\% \pm 2.85\%$ ,  $P = 0.01$ ). For the left circumflex artery (LCX) territory, the PI of all segments in patients with KD was lower than that of all segments in controls ( $9.87\% \pm 2.69\%$  vs.  $9.32\% \pm 2.39\%$  vs.  $10.57\% \pm 3.22\%$  vs.  $11.37\% \pm 3.07\%$ , respectively,  $P < 0.001$ ). The PI of segments subtended by normal CA in patients with CA dilation was lower than that of segments in patients without CA dilation and controls ( $P = 0.01$ , and  $P < 0.001$ , respectively). The Max SI of all segments in patients with KD decreased in the LAD, RCA, and LCX territories compared with that of segments in controls (all  $P < 0.001$ ). *Table 2* and *Figure S1* depict the LV regional perfusion parameters in detail. In addition, the diagnosis of KD was correlated with regional PI and Max SI (PI:  $r = -0.147$ ,  $P < 0.001$ ; Max SI:  $r = -0.161$ ,  $P < 0.001$ ).

### *Correlation between CA dilation and perfusion parameters*

The Z score was found to be significantly associated with

**Table 1** Baseline characteristics of KD patients and normal controls

Characteristics	Controls (n=37)	KD with CA dilation (n=40)	KD without CA dilation (n=37)	P value
Age (years)	6.19±3.32	6.07±3.20	5.32±2.27	0.47
Sex (male), n (%)	20 (54.1)	28 (70.0)	20 (54.1)	0.25
BMI (kg/m <sup>2</sup> )	16.18±2.42	15.91±2.20	15.67±1.40	0.59
Onset age (years)	N/A	4.94±3.21	4.56±2.11	0.58
IVIG treatment, n (%)	N/A	39 (97.5)	36 (97.3)	0.95
IVIG resistant, n (%)	N/A	14 (35.0)	13 (35.1)	0.99
LVEF (%)	59.73±5.96	59.48±8.44	56.57±7.87	0.23
LVEDV (mL)	59.36±18.51	62.22±21.47	62.79±20.93	0.63
LVESV (mL)	24.30±7.10	24.72±8.82	27.12±10.16	0.25
LVSV (mL)	35.06±12.24	37.80±14.45	35.67±12.71	0.70
CA dilation	–	–	–	–
CA dilation to small CAA, n (%)	N/A	9 (22.5)	N/A	N/A
Middle CAA, n (%)	N/A	16 (40.0)	N/A	N/A
Giant CAA, n (%)	N/A	15 (37.5)	N/A	N/A
Maximum diameter of CA artery (mm)	N/A	6.25 (4.63, 8.85)	2.62±0.38	<0.001
Z score	N/A	7.25 (5.05, 10.41)	1.14±0.65	<0.001
RCA and LCA dilation, n (%)	N/A	22 (55.0)	N/A	N/A
LCA dilation, n (%)	N/A	12 (30.0)	N/A	N/A
RCA dilation, n (%)	N/A	6 (15.0)	N/A	N/A
Follow-up treatment (n)	–	18	12	–
Antiplatelet, n (%)	N/A	17 (94.4)	6 (50.0)	0.01
Beta-blockers, n (%)	N/A	5 (27.8)	5 (41.7)	0.90
ACEI, n (%)	N/A	5 (27.8)	4 (33.3)	0.82
Anticoagulant, n (%)	N/A	7 (38.9)	0 (0)	0.008
Glucocorticoid, n (%)	N/A	2 (11.1)	2 (16.7)	0.94

Continuous variables are presented as mean ± standard deviation or interquartile range as appropriate. KD, Kawasaki disease; CA, coronary artery; BMI, body mass index; N/A, not applicable; IVIG, intravenous immunoglobulin; LVEF, left ventricular ejection fraction; LVEDV, left ventricular end-diastolic volume; LVESV, left ventricular end-systolic volume; LVSV, left ventricular stroke volume; CAA, coronary aneurysm; RCA, right coronary artery; LCA, left coronary artery; ACEI, angiotensin-converting enzyme inhibitor.

global PI in patients with CA dilation ( $r=-0.576$ ,  $P<0.001$ ). Meanwhile, the Z score was significantly associated with regional PI in segments subtended by dilated CA ( $r=-0.351$ ,  $P<0.001$ ). *Figure 5* presents the correlation between the Z score and PI in patients with CA dilation. However, it was not correlated with the global Max SI in patients with CA dilation ( $r=0.041$ ,  $P=0.81$ ) or regional Max SI in segments subtended by dilated CA ( $r=-0.081$ ,  $P=0.08$ ). In the

multivariate analysis adjusted for basic characteristics, illness onset and treatment, and CA dilation, the Z score was independently associated with a lower global PI ( $\beta=-0.409$ ,  $P=0.02$ , model  $R^2=0.170$ ) (*Table 3*).

#### *Change in perfusion parameters during follow-up*

A total of 30 patients, including 12 patients without CA

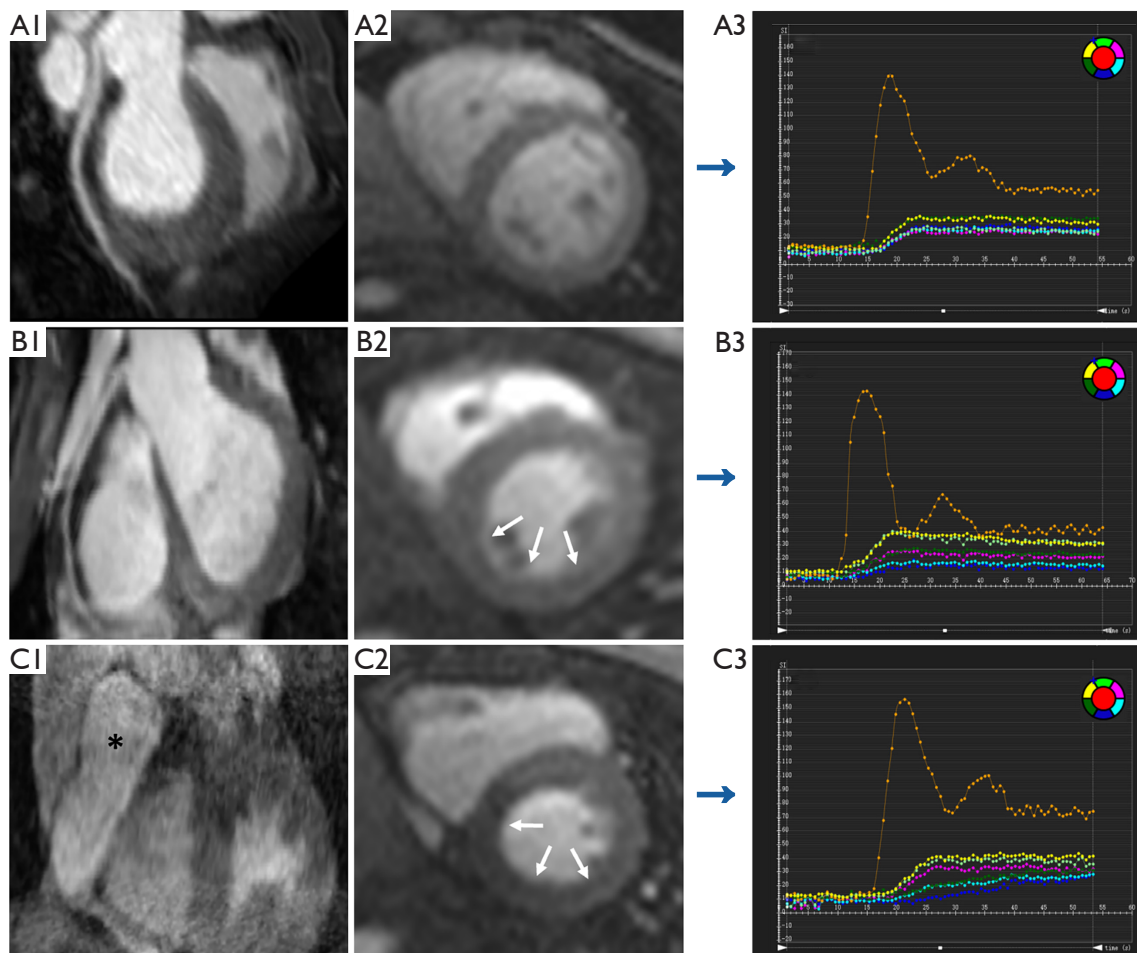


**Figure 3** Representative images of CMR myocardial first-pass perfusion in normal control, KD patients with and without CA dilation. (A1-A3) shows CMRA image of normal control (A1), no perfusion defect is found in any segment of LV (A2) and no significant decrease of Max SI was found (A3). (B1-B3) shows CMRA image of a patient without CA dilation (B1), subendocardial perfusion defect (B2) and decrease of Max SI (B3) is found at the inferior and posterior wall of the LV. (C1-C3) shows CMRA image of a patients with RCA dilation (inner diameter: 22.0 mm; Z score =17.97) (C1) and transmural perfusion defect (C2) and significant decrease of Max SI (C3) is found at posterior septum, inferior and posterior wall of LV. \*, location of RCA dilation. “Arrow” means perfusion defect. CMR, cardiac magnetic resonance; KD, Kawasaki disease; CA, coronary artery; CMRA, coronary magnetic resonance angiography; Max SI, maximum signal intensity; LV, left ventricular; RCA, right coronary artery.

dilation and 18 patients with CA dilation, completed the follow-up CMR with a median interval of 13 (IQR: 11.75, 16.25) months. The global Max SI of patients with and without CA dilation during the follow-up CMR decreased compared with that of the first CMR ( $42.18 \pm 9.84$  vs.  $34.48 \pm 8.24$ ,  $P=0.02$ ;  $44.82 \pm 7.13$  vs.  $36.61 \pm 7.67$ ,  $P=0.03$ , respectively); global PI of patients during follow-up CMR revealed a decreasing tendency compared with that of the first CMR, but without statistical significance ( $9.29 \pm 2.00$  vs.  $9.10 \pm 1.82$ ,  $P=0.78$ ;  $10.64 \pm 1.66$  vs.  $9.61 \pm 2.38$ ,  $P=0.15$ ,

respectively). The Z score during the first CMR was negatively correlated with the D-value of global PI between the first and follow-up CMR ( $r=-0.418$ ,  $P=0.02$ ). However, the Z score during the first CMR was not correlated with the D-value of global Max SI between the first and follow-up CMR ( $r=-0.103$ ,  $P=0.59$ ). In the multivariate analysis adjusted for basic characteristics, illness onset and treatment, and CA dilation, the Z score during the first CMR was negatively independently associated with the D-value of global PI between the first and follow-up CMR

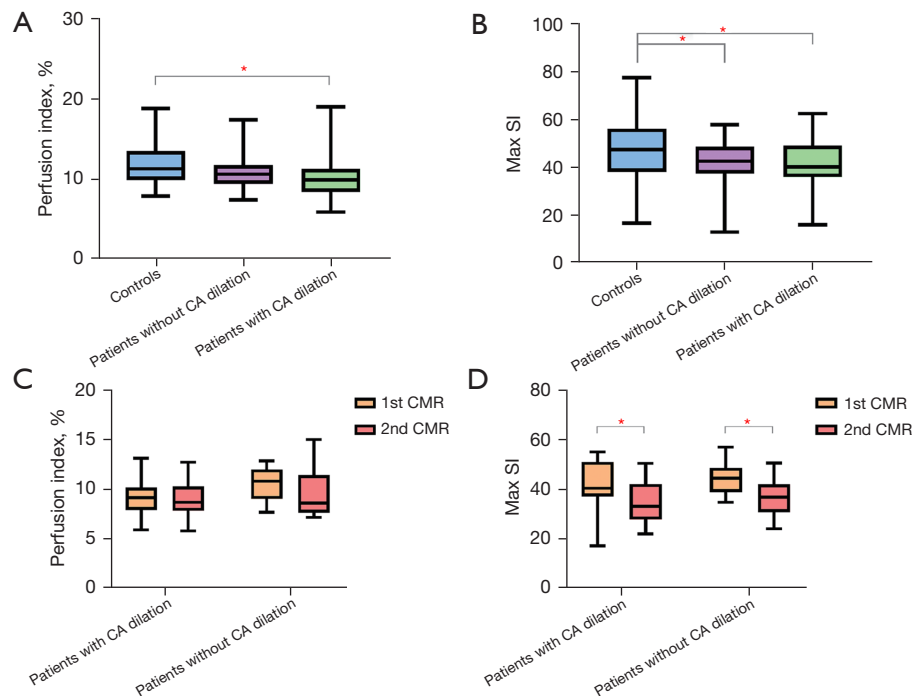


**Figure 4** Comparison of global perfusion parameters. (A,B) represents global perfusion parameters of KD patients during the first CMR. (C,D) represents global perfusion parameters of KD patients during the first and second CMR. \*, significant difference between any two groups. CA, coronary artery; Max SI, maximum signal intensity; KD, Kawasaki disease; CMR, cardiac magnetic resonance.

**Table 2** Comparison of regional perfusion parameters by coronary territory

Parameters	Controls	Segments of patients without CA dilation	Segments subtended by normal CA in patients with CA dilation	Segments subtended by dilated CA	P for trend
LAD	s=222	s=222	s=36	s=204	–
Perfusion index (%)	15.43±3.89	15.01±4.44	12.80±2.42 <sup>‡</sup>	13.86±4.14 <sup>‡</sup>	<0.001
Max SI	59.70±18.56	52.66±14.63*	50.19±14.13*	51.59±15.88*	<0.001
RCA	s=185	s=185	s=60	s=140	–
Perfusion index (%)	11.18±2.85	10.32±3.10*	11.98±5.38 <sup>‡</sup>	8.94±2.62 <sup>‡</sup>	<0.001
Max SI	43.23±12.69	36.78±9.95*	36.57±10.53*	36.65±11.34*	<0.001
LCX	s=185	s=185	s=70	s=130	–
Perfusion index (%)	11.37±3.07	10.57±3.22*	9.32±2.39 <sup>‡</sup>	9.87±2.69*	<0.001
Max SI	41.19±11.96	36.94±10.31*	37.59±10.68*	36.63±11.10*	<0.001

Data are expressed as mean ± SD. \*, P<0.05 vs. controls; <sup>‡</sup>, P<0.05 vs. segments of patients without CA dilation; <sup>#</sup>, P<0.05 vs. segments subtended by normal CA in patients with CA dilation. CA, coronary artery; LAD, left anterior descending artery; Max SI, maximum signal intensity; RCA, right coronary artery; LCX, left circumflex artery; SD, standard deviation; s, segments.

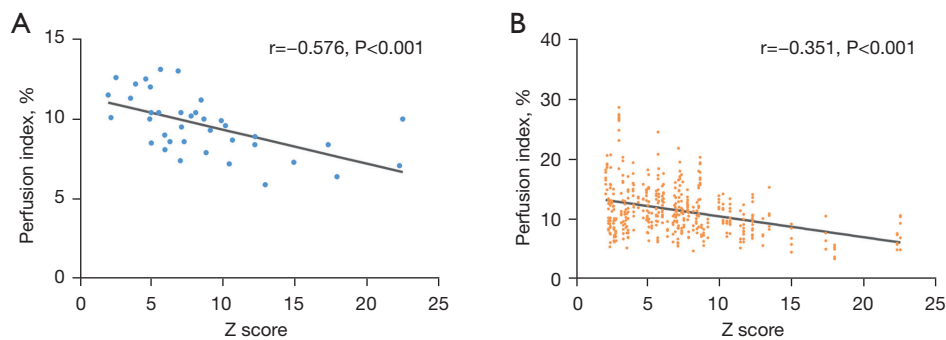


**Figure 5** Association of CA dilation with perfusion index. (A) a scatter plot of global PI and Z score in patients with CA dilation. (B) a scatter plot of regional PI and Z score in segments subtended by dilated CA. PI, perfusion index; CA, coronary artery.

**Table 3** Univariable and multivariable linear regression analysis of PI in KD patients (n=77)

Characteristics	Univariable		Multivariable <sup>a</sup>		
	$\beta$	P value	$\beta$	P value	R <sup>2</sup>
Age (years)	0.146	0.20	–	–	0.170
Sex	0.105	0.37	–	–	
BSA (m <sup>2</sup> )	0.192	0.10	0.174	0.11	
Onset age (years)	0.133	0.25	–	–	
IVIG resistance	0.129	0.27	–	–	
Course	0.012	0.92	–	–	
No. of CA dilation	-0.238	0.04	-0.061	0.71	
Z score	-0.368	0.001	-0.409	0.02	

<sup>a</sup>, candidate variables for multivariable model were selected on clinical characteristics and CA dilation, guided by univariable correlation with P value <0.10 and the absence of collinearity. PI, perfusion index; KD, Kawasaki disease; BSA, body surface area; IVIG, intravenous immunoglobulin; CA, coronary artery.

( $\beta=-0.162$ ,  $P=0.03$ , model  $R^2=0.386$ ) (Table S1).

There were 11 patients who underwent the first CMR in the acute phase and 19 patients who underwent the first CMR in the chronic phase. There was no difference in PI and Max SI between the first and follow-up CMR in patients underwent the first CMR in acute phase [9.30 (7.30, 10.70) vs. 9.60 (7.43, 12.13),  $P=0.93$ ; 40.75 (40.05, 51.22) vs. 42.07 (32.72, 44.04),  $P=0.51$ , respectively]. The PI and Max SI of the follow-up CMR decreased when compared to the first CMR in patients underwent the first CMR at chronic phase (10.22±1.86 vs. 8.85±1.37,  $P=0.01$ ; 42.90±9.36 vs. 32.78±7.24,  $P=0.001$ , respectively).

### Reproducibility of perfusion parameters

Regarding the reproducibility of perfusion parameters, there were good intra- and interobserver agreements in global PI [ICC =0.855 (95% CI: 0.670–0.940) and 0.819 (95% CI: 0.599–0.924), respectively] and excellent intra- and interobserver agreements in global Max SI [ICC =0.992 (95% CI: 0.979–0.997) and 0.956 (95% CI: 0.893–0.982), respectively].

### Discussion

This study showed that the global and regional Max SI of patients with and without CA dilation decreased compared with those of controls. Moreover, the global Max SI continually decreased during the first and follow-up CMR. The global PI of patients with CA dilation and regional PI in segments subtended by dilated CA were lower than that of controls. Further, it was negatively correlated with the Z score. Finally, the Z score during the first CMR was an independent predictor of global PI reduction at the first CMR and the D-value of global PI between the first and follow-up CMR in patients with KD. The first-pass perfusion CMR can facilitate the semi-quantitative evaluation of myocardial perfusion impairment in KD. Myocardial perfusion impairment was observed not only in patients with CA dilation but also in those without. Meanwhile, it exists not only in the segments subtended by dilated CA but also in the myocardial segments subtended by non-dilated CA. CA dilation was independently correlated with myocardial perfusion impairment. In addition, patients with KD had decreased perfusion parameters over time, which were correlated with the Z score during the first CMR.

Our study showed that decreased global and regional Max SI, regardless of epicardial CA lesions, demonstrated impaired myocardial perfusion existed commonly in patients with KD. This finding is consistent with previous reports on PET (10), SPECT (5), and CMR (6,7). Excluding the patients with CA thrombosis and/or stenosis in the epicardial CA, the myocardial perfusion impairment may be caused by myocardial microcirculation dysfunction, which maybe contribute to endothelial dysfunction and diffuse myocardial fibrosis (6,11). The pathological changes in CA inflammation, including inflammatory cell infiltration in CA intima, chronic extracellular matrix remodeling and myofibroblastic proliferation, can cause CA intima thickening and endothelial dysfunction (5,11,19). Endothelial dysfunction may cause the abnormalities in mechanism of regulating myocardial perfusion, leading to myocardial microcirculation dysfunction. In addition, myocarditis is observed in almost all patients with KD in the acute stage, which also exists in the follow-up phase and leads to myocardial fibrosis (20-24). Interstitial and perivascular fibrosis and extravascular compression of microcirculatory vessels caused by myocardial fibrosis may affect myocardial microcirculation dysfunction (14,25). At present, there is no study on the prognostic value of myocardial microcirculation dysfunction in patients with KD. However, myocardial microcirculation dysfunction has been identified as a prognostic value for the prediction of cardiovascular events in cardiovascular diseases such as cardiomyopathy and coronary artery disease (26,27). We will further explore the prognostic value of myocardial microcirculation dysfunction in KD in the next stage.

We found that the regional Max SI and PI decreased in segments subtended by normal CA in patients with CA dilation and segments of patients without CA dilation. This supports the premise that myocardial microcirculation dysfunction may exist widely in patients with KD (6,7). Several studies based on stress myocardial perfusion of KD have shown that myocardial flow reserve of all of patients with KD was decreased compared with that of controls (4,6,7,10). However, the myocardial blood flow of patients with KD at rest did not differ from that of controls (4,10). The lack of consensus on rest myocardial perfusion in the literature may be a reflection of the small sample sizes, older age of controls, and different approaches in these studies (4,10). Nevertheless, our study had significant advantages compared with previous CMR perfusion studies with a larger sample size and age- and sex-matched controls. Notably, the PI of segments subtended by normal CA in

patients with CA dilation was lower than that of segments in patients without CA dilation and controls in the LAD and LCX territories. A previous study showed that patients with CA lesions in the LAD and LCX arteries had significant perfusion attenuation in segments subtended by the 2 arteries compared with controls (7). Hence, the myocardial microcirculation in the LCA territory of KD may be more vulnerable.

In this study, the global PI of patients with CA dilation and regional PI in segments subtended by dilated CA decreased. CA dilation was negatively correlated with global and regional PI in KD patients with CA dilation, and CA dilation was an independent predictor of global PI. PI is the ratio of upslope<sub>max</sub> in the myocardium and upslope<sub>max</sub> in the LV blood pool. Individual factors affecting PI, such as contrast agent dose, contrast injection speed, and evacuation speed, can be excluded. PI reflected the wash-in of myocardial microcirculation (28-30). The analysis of image-based modeling of hemodynamics in CA aneurysm based on coronary computed tomography angiography showed flow recirculation and reduced wall shear stress within the aneurysm and high wall shear stress gradients at the aneurysm neck (31). The energy loss caused by turbulence in the CA aneurysm is similar to that of coronary stenosis (32). This can result in decreased epicardial coronary inflow velocity and can further reduce the wash-in of myocardial microcirculation.

Interestingly, the global Max SI of patients with CA dilation and regional Max SI in segments subtended by dilated CA were not correlated with the Z score in our study. However, the diagnosis of KD was negatively associated with the global and regional Max SI. This may indicate that KD is an influencing factor of Max SI reduction. CA dilation primarily decreased wash-in flow velocity. Ultimately, it has minimal impact on Max SI. Hence, there was no significant correlation between Max SI and CA dilation.

In 30 patients who completed the follow-up CMR, the global Max SI of patients with and without CA dilation during the second follow-up CMR decreased compared with that of the first CMR. The PI and Max SI of the follow-up CMR decreased compared to the first CMR in patients who underwent the first CMR during the chronic phase. Thus, patients with KD who presented with CA dilation and those without were at risk for worse myocardial perfusion impairment during follow-up, especially the patients who underwent the first CMR in the chronic phase. In addition, the Z score during the first CMR was negatively associated

with the D-value of global PI between the first and follow-up CMR. A study based on the semi-quantitative assessment of myocardial perfusion using CMR in KD showed that 3 (50%) patients with decreased myocardial perfusion in the follow-up evaluation had thrombus or severe CA stenosis at the initial echocardiography evaluation (7). We included a larger sample to validate that the same trend also existed in patients with and without CA dilation.

The current study had several limitations, which should be addressed. First, it was performed at a single center, and the recruitment of patients was based in a large tertiary referral hospital. Hence, the study may be subject to referral bias. In addition, the impact of myocardial perfusion impairment on the clinical manifestations and prognosis of KD needs follow-up data, and we will further acquire this data in the future. Further, the participants in this study did not undergo myocardial perfusion with stress CMR. However, the study results found that the rest myocardial perfusion of patients with KD was lower than that of controls, which could reflect the myocardial perfusion impairment of KD. We speculated that the widespread decrease of myocardial perfusion in patients with KD may be due to the myocardial microcirculation dysfunction by excluding the CA thrombosis and/or stenosis of epicardial coronary arteries. Moreover, stress CMR myocardial perfusion could increase the risk of side effects related to stress agent (33,34).

## Conclusions

Myocardial first-pass perfusion CMR could semi-quantitatively evaluate myocardial perfusion impairment in patients with KD. Not only patients with CA dilation and segments subtended by dilated CA, but also those without CA dilation and segments subtended by non-dilated CA, developed myocardial perfusion impairment; the severity of myocardial perfusion impairment is associated with the degree of CA dilation. These findings may help to elucidate the characteristics of myocardial injuries in KD and to detect subclinical myocardial ischemia in KD, which could potentially serve as an imaging marker for follow-up and efficacy evaluation of treatment of KD.

## Acknowledgments

**Funding:** This work was supported by Operating Funds of Molecular Imaging Laboratory of Southwest Institute of Maternity and Child Research (Fund No. K1519); National

Natural Science Foundation of China (Nos. 82071874, 82120108015, 82102020, and 82271981); and Sichuan Science and Technology Program (Nos. 2020YJ0029, 21ZDYF1967, 2023YFS0020, and 2021YFS0175).

## Footnote

**Reporting Checklist:** The authors have completed the STROBE reporting checklist. Available at <https://qims.amegroups.com/article/view/10.21037/qims-23-1802/rc>

**Conflicts of Interest:** All authors have completed the ICMJE uniform disclosure form (available at <https://qims.amegroups.com/article/view/10.21037/qims-23-1802/coif>). The authors have no conflicts of interest to declare.

**Ethical Statement:** The authors are accountable for all aspects of the work in ensuring that questions related to the accuracy or integrity of any part of the work are appropriately investigated and resolved. The study was conducted in accordance with the Declaration of Helsinki (as revised in 2013), and has been approved by Medical Ethics Committee of Sichuan University (No. K2019058). Written informed consent was provided by the parents of all patients in this study.

**Open Access Statement:** This is an Open Access article distributed in accordance with the Creative Commons Attribution-NonCommercial-NoDerivs 4.0 International License (CC BY-NC-ND 4.0), which permits the non-commercial replication and distribution of the article with the strict proviso that no changes or edits are made and the original work is properly cited (including links to both the formal publication through the relevant DOI and the license). See: <https://creativecommons.org/licenses/by-nc-nd/4.0/>.

## References

1. Burns JC, Glodé MP. Kawasaki syndrome. *Lancet* 2004;364:533-44.
2. McCrindle BW, Rowley AH, Newburger JW, Burns JC, Bolger AF, Gewitz M, Baker AL, Jackson MA, Takahashi M, Shah PB, Kobayashi T, Wu MH, Saji TT, Pahl E; American Heart Association Rheumatic Fever, Endocarditis, and Kawasaki Disease Committee of the Council on Cardiovascular Disease in the Young; Council on Cardiovascular and Stroke Nursing; Council on Cardiovascular Surgery and Anesthesia; and Council on

- Epidemiology and Prevention. Diagnosis, Treatment, and Long-Term Management of Kawasaki Disease: A Scientific Statement for Health Professionals From the American Heart Association. *Circulation* 2017;135:e927-99.
3. Fukazawa R, Kobayashi J, Ayusawa M, Hamada H, Miura M, Mitani Y, et al. JCS/JSCS 2020 Guideline on Diagnosis and Management of Cardiovascular Sequelae in Kawasaki Disease. *Circ J* 2020;84:1348-407.
  4. Hauser M, Bengel F, Kuehn A, Nekolla S, Kaemmerer H, Schwaiger M, Hess J. Myocardial blood flow and coronary flow reserve in children with "normal" epicardial coronary arteries after the onset of Kawasaki disease assessed by positron emission tomography. *Pediatr Cardiol* 2004;25:108-12.
  5. Cicala S, Pellegrino T, Storto G, Caprio MG, Paladini R, Mainolfi C, de Leva F, Cuocolo A. Noninvasive quantification of coronary endothelial function by SPECT imaging in children with a history of Kawasaki disease. *Eur J Nucl Med Mol Imaging* 2010;37:2249-55.
  6. Bratis K, Chiribiri A, Hussain T, Krasemann T, Henningsson M, Phinikaridou A, Mavrogeni S, Botnar R, Nagel E, Razavi R, Greil G. Abnormal myocardial perfusion in Kawasaki disease convalescence. *JACC Cardiovasc Imaging* 2015;8:106-8.
  7. Friesen RM, Schäfer M, Jone PN, Appiawiah N, Vargas D, Fonseca B, DiMaria MV, Truong U, Malone L, Browne LP. Myocardial Perfusion Reserve Index in Children With Kawasaki Disease. *J Magn Reson Imaging* 2018;48:132-9.
  8. Muthusami P, Luining W, McCrindle B, van der Geest R, Riesenkampff E, Yoo SJ, Seed M, Manlhiot C, Grosse-Wortmann L. Myocardial Perfusion, Fibrosis, and Contractility in Children With Kawasaki Disease. *JACC Cardiovasc Imaging* 2018;11:1922-4.
  9. Hamaoka K, Onouchi Z, Kamiya Y, Sakata K. Evaluation of coronary flow velocity dynamics and flow reserve in patients with Kawasaki disease by means of a Doppler guide wire. *J Am Coll Cardiol* 1998;31:833-40.
  10. Furuyama H, Odagawa Y, Katoh C, Iwado Y, Yoshinaga K, Ito Y, Noriyasu K, Mabuchi M, Kuge Y, Kobayashi K, Tamaki N. Assessment of coronary function in children with a history of Kawasaki disease using (15)O-water positron emission tomography. *Circulation* 2002;105:2878-84.
  11. Furuyama H, Odagawa Y, Katoh C, Iwado Y, Ito Y, Noriyasu K, Mabuchi M, Yoshinaga K, Kuge Y, Kobayashi K, Tamaki N. Altered myocardial flow reserve and endothelial function late after Kawasaki disease. *J Pediatr* 2003;142:149-54.
  12. Tsuno K, Fukazawa R, Kiriya T, Imai S, Watanabe M, Kumita S, Itoh Y. Peripheral Coronary Artery Circulatory Dysfunction in Remote Stage Kawasaki Disease Patients Detected by Adenosine Stress <sup>13</sup>N-Ammonia Myocardial Perfusion Positron Emission Tomography. *J Clin Med* 2022;11:1134.
  13. Feher A, Sinusas AJ. Quantitative Assessment of Coronary Microvascular Function: Dynamic Single-Photon Emission Computed Tomography, Positron Emission Tomography, Ultrasound, Computed Tomography, and Magnetic Resonance Imaging. *Circ Cardiovasc Imaging* 2017;10:e006427.
  14. Schindler TH, Dilsizian V. Coronary Microvascular Dysfunction: Clinical Considerations and Noninvasive Diagnosis. *JACC Cardiovasc Imaging* 2020;13:140-55.
  15. Azhe S, Li X, Zhou Z, Fu C, Wang Y, Zhou X, An J, Piccini D, Bastiaansen J, Guo Y, Wen L. Comparison between diaphragmatic-navigated and self-navigated coronary magnetic resonance angiography at 3T in pediatric patients with congenital coronary artery anomalies. *Quant Imaging Med Surg* 2024;14:61-74.
  16. Cerqueira MD, Weissman NJ, Dilsizian V, Jacobs AK, Kaul S, Laskey WK, Pennell DJ, Rumberger JA, Ryan T, Verani MS; American Heart Association Writing Group on Myocardial Segmentation and Registration for Cardiac Imaging. Standardized myocardial segmentation and nomenclature for tomographic imaging of the heart. A statement for healthcare professionals from the Cardiac Imaging Committee of the Council on Clinical Cardiology of the American Heart Association. *Circulation* 2002;105:539-42.
  17. Kobayashi T, Fuse S, Sakamoto N, Mikami M, Ogawa S, Hamaoka K, Arakaki Y, Nakamura T, Nagasawa H, Kato T, Jibiki T, Iwashima S, Yamakawa M, Ohkubo T, Shimoyama S, Aso K, Sato S, Saji T; Z Score Project Investigators. A New Z Score Curve of the Coronary Arterial Internal Diameter Using the Lambda-Mu-Sigma Method in a Pediatric Population. *J Am Soc Echocardiogr* 2016;29:794-801.e29.
  18. Koo TK, Li MY. A Guideline of Selecting and Reporting Intraclass Correlation Co-efficients for Reliability Research. *J Chiropr Med* 2016;15:155-63.
  19. Orenstein JM, Shulman ST, Fox LM, Baker SC, Takahashi M, Bhatti TR, Russo PA, Mierau GW, de Chadarevian JP, Perlman EJ, Trevenen C, Rotta AT, Kalelkar MB, Rowley AH. Three linked vasculopathic processes characterize Kawasaki disease: a light and transmission electron microscopic study. *PLoS One* 2012;7:e38998.

20. Gorelik M, Lee Y, Abe M, Andrews T, Davis L, Patterson J, Chen S, Crother TR, Aune GJ, Noval Rivas M, Arditi M. IL-1 receptor antagonist, anakinra, prevents myocardial dysfunction in a mouse model of Kawasaki disease vasculitis and myocarditis. *Clin Exp Immunol* 2019;198:101-10.
21. Harada M, Yokouchi Y, Oharaseki T, Matsui K, Tobayama H, Tanaka N, Akimoto K, Takahashi K, Kishihiro M, Shimizu T, Takahashi K. Histopathological characteristics of myocarditis in acute-phase Kawasaki disease. *Histopathology* 2012;61:1156-67.
22. Yutani C, Go S, Kamiya T, Hirose O, Misawa H, Maeda H, Kozuka T, Onishi S. Cardiac biopsy of Kawasaki disease. *Arch Pathol Lab Med* 1981;105:470-3.
23. Hoshino S, Shimizu C, Jain S, He F, Tremoulet AH, Burns JC. Biomarkers of Inflammation and Fibrosis in Kawasaki Disease Patients Years After Initial Presentation With Low Ejection Fraction. *J Am Heart Assoc* 2020;9:e014569.
24. Yao Q, Hu XH, He LL. Evaluation of comprehensive myocardial contractility in children with Kawasaki disease by cardiac magnetic resonance in a large single center. *Quant Imaging Med Surg* 2022;12:481-92.
25. Crea F, Camici PG, Bairey Merz CN. Coronary microvascular dysfunction: an update. *Eur Heart J* 2014;35:1101-11.
26. Bom MJ, van Diemen PA, Driessen RS, Everaars H, Schumacher SP, Wijmenga JT, Raijmakers PG, van de Ven PM, Lammertsma AA, van Rossum AC, Knuuti J, Danad I, Knaapen P. Prognostic value of [15O]H<sub>2</sub>O positron emission tomography-derived global and regional myocardial perfusion. *Eur Heart J Cardiovasc Imaging* 2020;21:777-86.
27. Thomas M, Sperry BW, Peri-Okonny P, Malik AO, McGhie AI, Saeed IM, Chan PS, Spertus JA, Thompson RC, Bateman TM, Patel KK. Relative Prognostic Significance of Positron Emission Tomography Myocardial Perfusion Imaging Markers in Cardiomyopathy. *Circ Cardiovasc Imaging* 2021;14:e012426.
28. Yang MX, Li QL, Wang DQ, Ye L, Li KM, Lin XJ, Li XS, Fu C, Ma XM, Guo YK, Yin RT, Yang ZG. Myocardial microvascular function assessed by CMR first-pass perfusion in patients treated with chemotherapy for gynecologic malignancies. *Eur Radiol* 2022;32:6850-8.
29. Xu HY, Yang ZG, Sun JY, Wen LY, Zhang G, Zhang S, Guo YK. The regional myocardial microvascular dysfunction differences in hypertrophic cardiomyopathy patients with or without left ventricular outflow tract obstruction: assessment with first-pass perfusion imaging using 3.0-T cardiac magnetic resonance. *Eur J Radiol* 2014;83:665-72.
30. Liu X, Yang ZG, Gao Y, Xie LJ, Jiang L, Hu BY, Diao KY, Shi K, Xu HY, Shen MT, Ren Y, Guo YK. Left ventricular subclinical myocardial dysfunction in uncomplicated type 2 diabetes mellitus is associated with impaired myocardial perfusion: a contrast-enhanced cardiovascular magnetic resonance study. *Cardiovasc Diabetol* 2018;17:139.
31. Sengupta D, Kahn AM, Burns JC, Sankaran S, Shadden SC, Marsden AL. Image-based modeling of hemodynamics in coronary artery aneurysms caused by Kawasaki disease. *Biomech Model Mechanobiol* 2012;11:915-32.
32. Murakami T, Tanaka N. The physiological significance of coronary aneurysms in Kawasaki disease. *EuroIntervention* 2011;7:944-7.
33. Cerqueira MD, Verani MS, Schwaiger M, Heo J, Iskandrian AS. Safety profile of adenosine stress perfusion imaging: results from the Adenoscan Multicenter Trial Registry. *J Am Coll Cardiol* 1994;23:384-9.
34. Layland J, Carrick D, Lee M, Oldroyd K, Berry C. Adenosine: physiology, pharmacology, and clinical applications. *JACC Cardiovasc Interv* 2014;7:581-91.

**Cite this article as:** Zhou Z, Zhang N, Azhe S, Hu L, Peng S, Guo Y, Zhou K, Wang C, Wen L. Myocardial perfusion impairment in children with Kawasaki disease: assessment with cardiac magnetic resonance first-pass perfusion. *Quant Imaging Med Surg* 2024;14(7):4923-4935. doi: 10.21037/qims-23-1802